OPTICAL WAVEFRONT ANALYSIS OF THERMALLY CYCLED 500 MM METALLIC MIRRORS

L. Noethe, F. Franza, P. Giordano, R. Wilson
European Southern Observatory
Karl-Schwarzschild-Str. 2
D-8046 Garching

1. Aim of the experiment

Warping is a major concern in the use of aluminium as a material for large mirrors. The warping characteristics are influenced by:

* the type of material, i.e. pure aluminium or some alloy
* the type of fabrication, i.e. cast, rolled or forged.

So far there is little data available on the warping characteristics of aluminium mirrors. Therefore ESO has tested the warping behaviour of 18 aluminium mirrors under thermal cycling conditions with a glass ceramic mirror, which has not been cycled, as a reference mirror. The set of 500 mm mirrors selected for this experiment is described in [1].

2. Thermal Cycling Procedure

Two test mirrors are always thermally cycled together with a dummy mirror of approximately the same size as the test mirrors. The temperatures are monitored in the centre and near the surface of the dummy mirror. The temperatures are changed as quickly as possible. The sequence of sets of thermal cycles applied to each mirror is indicated in Fig. 1.

(a) One soft cycle with a temperature range from -5 to 25 degrees centigrade.

(b) Seven sets of hard cycles such that after n sets of cycles a total of m cycles has been performed.

n :	1	2	3	4	5	6	7
m :	1	2	4	8	16	32	50

The temperature range is -20 to +50 degrees centigrade.

(c) One very hard cycle with a temperature range from -30 to +90 degrees centigrade.

Proceedings of the IAU Colloquium No. 79: "Very Large Telescopes, their Instrumentation and Programs", Garching, April 9–12, 1984.

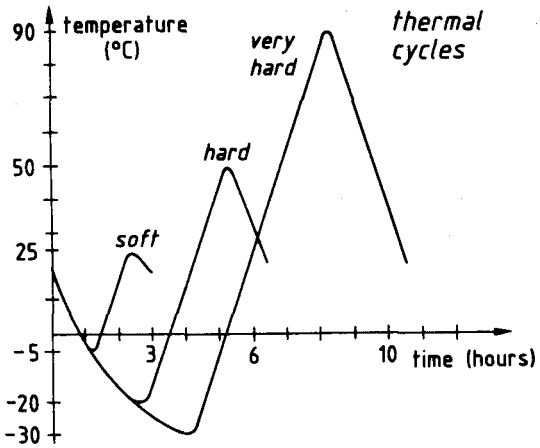

Figure 1: Temperature in the centre of the dummy mirror during the three types of thermal cycles.

For all cycles the temperature gradients are approximately 20 degrees centigrade per hour and approx. 1 degree centigrade between the centre and the surface of the mirror.

After each set of cycles the mirrors are tested optically.

2. Types of deformations to be detected in the experiment

In the optical analysis those types of surface deformations and therefore wavefront aberrations are investigated which can most easily be corrected by active optics. The coefficients (b to h together with the angles θ_0 to θ_4) of the various types of aberrations are obtained by fitting the data of a Shack-Hartmann test to the following quasi-Zernike polynomial.

$$
\begin{aligned}
W(r,\phi) = \quad & a \\
& + b\, r \cos(\phi + \theta_0) && \text{tilt} \\
& + c\, r^2 && \text{longitudinal focus} \\
& + d\, r^3 \cos(\phi + \theta_1) && \text{3rd order coma} \\
& + e\, r^4 && \text{3rd order spherical aberration} \\
& + f\, r^2 \cos(2\phi + \theta_2) && \text{3rd order astigmatism} \\
& + g\, r^3 \cos(3\phi + \theta_3) && \text{triangular coma} \\
& + h\, r^4 \cos(4\phi + \theta_4) && \text{quadratic astigmatism}
\end{aligned}
$$

https://doi.org/10.1017/S0252921100108279 Published online by Cambridge University Press

3. Optical test procedure

(a) All mirrors are tested before the thermal cycling and after each set of thermal cycles.

(b) We use the Shack-Hartmann test. The set-up of the experiment is shown in Fig. 2.

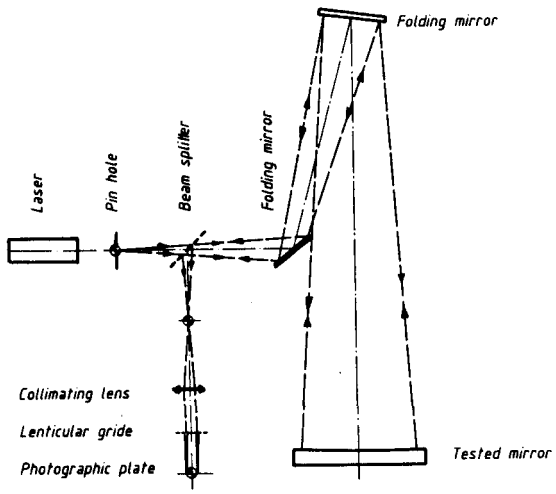

Figure 2: Set-up of the Shack-Hartmann experiment

The following points should be noted:

* The test set-up adds fixed aberrations (beam splitter and the two plane mirrors) to the aberrations of the test mirrors.

* Focussing is done by moving the Shack-Hartmann device. No measurement of the change of the radius of curvature has been done and all coefficients are obtained from the calculation for the position of best focus.

* In contrast to the test of a telescope where third order coma due to a deformation of the surface of the mirror cannot be distinguished from the third order coma due to the relative orientation of the axes of the primary and secondary mirror, we can with this test set-up measure third order coma produced by the surface of the test mirror.

https://doi.org/10.1017/S0252921100108279 Published online by Cambridge University Press

* The accuracy of the analysis is influenced by:

- air turbulences
- the process of taking the photographic plates
- the digitization of the plates

(these three effects give rise to statistical noise)

- changes in the test set-up.

(c) Each mirror is rotated around its optical axis and is measured at six different angles ranging from 0 to 150 degrees during each optical test. This procedure offers two advantages:

- a reduction of the statistical noise because of the higher number of measurements
- possibility to separate for all aberrations with an azimuth dependence (i.e. all aberrations except all types of spherical aberration) the fixed aberrations produced by the system from the aberrations produced by the mirror. Any change in the test set-up will therefore only affect the coefficients of spherical aberration.

(d) Test of a supposedly stable glass ceramic mirror at regular time intervals to monitor the stability of the test set-up. With this test we can check if changes in the coefficients of any type of spherical aberration are caused by changes in the test set-up.

(4) Results

As the aim of the experiment is the comparison of the warping behaviour of various aluminium mirrors, conclusions should be drawn only after all mirrors have been tested. Therefore we will, at the present stage of the experiment, just present some data to show

(a) the accuracy with which we can detect changes of the coefficients under laboratory conditions and

(b) that our thermal cycling procedure does reveal differences in the warping behaviour of the test mirrors.

Figure 3 shows the coefficients of the non-cycled glass ceramic mirror for seven

https://doi.org/10.1017/S0252921100108279 Published online by Cambridge University Press

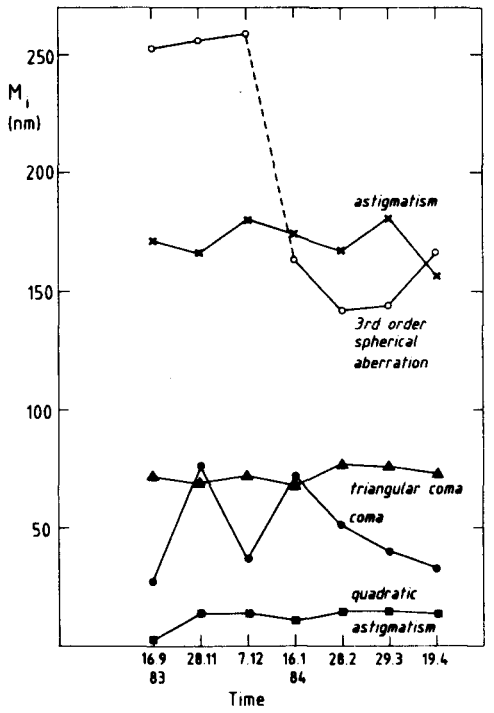

Figure 3: Magnitudes Mi of the coefficients of the wavefront aberration of the glass ceramic mirror

different measurements over a period of 7 months. The jump of approximately 100 nm of the coefficient of third order spherical aberration is due to a change in the test set-up. All the other azimuth dependent coefficients do not show such a jump because the effect of the change of the fixed aberrations of the test system can be eliminated by the rotation of the mirror.

Roughly speaking, one can say that the coefficients of spherical aberration and coma can be measured with an accuracy of at least 50 nm and the coefficients of astigmatism, triangular coma and quadratic astigmatism with an accuracy of 20 nm.

In the following drawings we shall use the following indices:

i : initial measurement

s : measurement after the soft cycle

1,2,4,8,16,32,50 : measurement after a total of 1,2,4,8,16,32,50 hard cycles

vh : measurement after the very hard cycle

https://doi.org/10.1017/S0252921100108279 Published online by Cambridge University Press

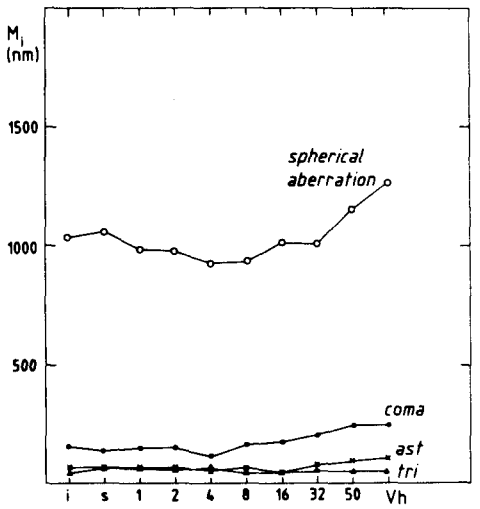

Fig. 4: magnitudes of the coefficients of the wavefront aberrations of mirror A

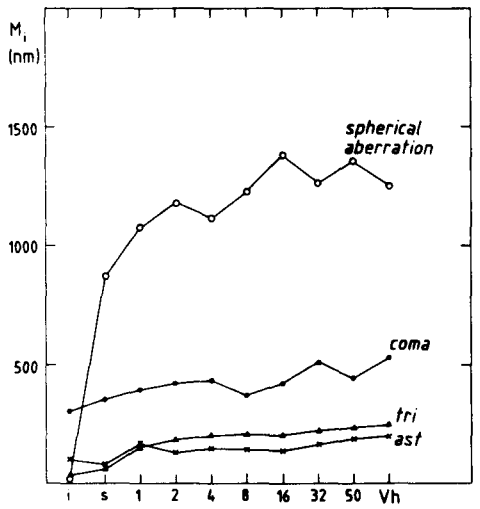

Fig. 5: magnitudes of the coefficients of the wavefront aberrations of mirror B

Figures 4 and 5 show the evolution of the magnitudes of spherical aberration, coma, astigmatism and triangular coma for two mirrors A and B which were always cycled together. It is apparent, that A is stable in the beginning but shows some minor warping after the completion of 50 hard cycles and the very hard cycle, whereas B shows significant changes during the first set of cycles but stabilizes during the cycling test. This could be an effect which one would expect for a process of stress release during thermal treatment.

The most significant changes appear in the spherical aberration mode. Therefore we plot the wavefront aberration as a function of the radius only, i.e. after an integration over the azimuth angle.

$$W(r) = \frac{1}{2\pi} \int_0^{2\pi} W(r,\phi)\, d\phi$$

This function should give a more complete picture of the warping behaviour in the rotationally symmetric mode than the coefficient of third order spherical aberration which is obtained by fitting the function r^4 to W(r).

https://doi.org/10.1017/S0252921100108279 Published online by Cambridge University Press

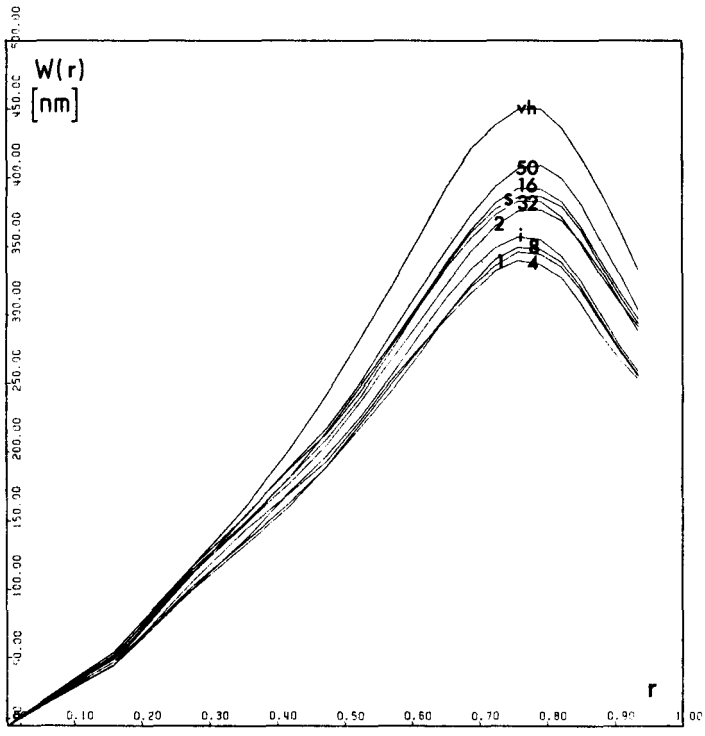

Figure 6: Rotationally symmetric part of the wavefront aberration of mirror A.

Figures 6 and 7 show W(r) for the two mirrors mentioned above for the position of best focus.

It can be seen that mirror A has warped significantly only after the very hard cycle. Nevertheless, the maximum variation of the wavefront aberration is small.

In contrast, mirror B has warped already during the soft cycle but it has been stable after the completion of 16 hard cycles. A small change of the same order of magnitude as in the case of mirror A did occur after the very hard cycle.

https://doi.org/10.1017/S0252921100108279 Published online by Cambridge University Press

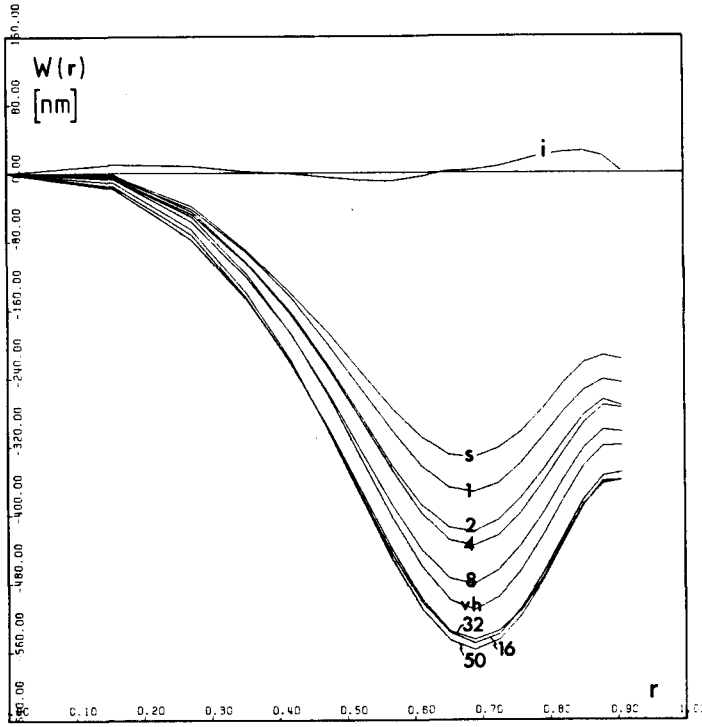

Figure 7: Rotationally symmetric part of the wavefront aberration of mirror B.

References

1. K.N. Mischung, "ESO's New Technology Telescope (NTT), Metallic Primary Mirror Project", Proc. of IAU Conference No. 79, ESO Garching, April 1984.

DISCUSSION

R. Wilson: (to J. Nelson in response to a question addressed to L. Noethe) All the evidence available confirms that warping occurs in the low spatial frequency modes which we are specifically analysing, not in high spatial frequency modes like ripple. With the SHACK-HARTMANN test, we can nevertheless detect variation in ripple by variation in the "intrinsic quality" - the energy concentration after removal of the low frequency terms. We can also detect it directly by comparison of initial and final interferograms.

https://doi.org/10.1017/S0252921100108279 Published online by Cambridge University Press